

# Characterization and Preparation of Metallic Nanoparticles Decorated Graphene Oxide/ Carbon Nanotube on Polytetrafluoroethylene Membrane as an electrochemical Filter for Wastewater Treatment

Xianliang Li<sup>1\*</sup>, Tao Xia<sup>2</sup>

<sup>1</sup> College of Bioengineering, Jingchu University of Science and Technology, Jingmen 448000, China

<sup>2</sup> School of life sciences, Huazhong Agricultural University, Wuhan 430071, China

\*E-mail: [lixianling163@sina.com](mailto:lixianling163@sina.com)

*Received:* 30 March 2020 / *Accepted:* 19 May 2020 / *Published:* 10 July 2020

---

Nowadays, the increasing demand and the reduction of sources of drinking water are the big challenges for all industries. Therefore, studying and designing a high efficiency wastewater treatment device is essential. In this work, graphene oxide (GOx), Au nanoparticles decorated graphene oxide (AuGOx) and Ag nanoparticles decorated graphene oxide (AgGOx) electrode was applied to electro-oxidation of tetracycline, phenol and oxalate from both of deionized and real water samples. The GOx, AuGOx and AgGOx structures were synthesized through chemical approach. The structural properties of synthesized GOx, AuGOx and AgGOx were studied by FESEM and XRD. Results showed that the prepared structures had high density, aspect ratio and porosity. Electrochemical properties of filters were investigated by differential pulse voltammetry (DPV), electrochemical impedance spectroscopy and chronoamperometry techniques. The result showed that AgGOx/CNTs filter exhibited higher electro-oxidation rate than GOx, AuGOx filters. The DPV findings indicated that AgGOx/CNTs can be the proposed filter to remove phenol from real wastewater samples.

---

**Keywords:** Metallic nanoparticles; Graphene oxide electrode; Wastewater treatment; Differential pulse voltammetry

## 1. INTRODUCTION

The increasing world population and the improvement in the standard of living and health has led to an increasing demand of water [1]. Global warming and environmental pollution, especially underground, through industrial wastewater leads to a reduction of fresh water sources [2]. In addition, one of industry challenges is the development of green technologies to reuse water and reducing of waste. Wastewater treatment is one of important approaches to save the sources of drinking waters [3].

The purification of wastewater prepares the required irrigation water in agriculture industry. Some essential problems in designing of the filters are low absorption ability, high cost, low stability, time-consuming and huge architecture. Therefore, optimizing and modifying of filters is necessary [4].

Today, nanotechnology can improve the design and structure of instruments through the miniaturization and promotion the surface related properties such as hydrophobia [1], optical [5, 6], catalytic [7], reactivity and chemical the physical absorption [8, 9]. On the other hand, modification of the active surface of filters by nanomaterials can enhance the performance and efficiency of treatment operations because of the high aspect ratio and high porosity of nanostructures [10].

Graphene, a new structure of carbon, exhibits a considerable attention in the last decade because of its outstanding properties such as high electrical conductivity, large effective surface area, super hydrophobicity and high chemical activity [11, 12]. Graphene is considered as environmentally friendly material that extensively used in electronic, biomedicine and energy saving composites industries [13, 14]. Although, studies showed that the decoration or modification the graphene sidewalls with metallic ions exhibited the special chemical and physical properties for application in wastewater treatment [15, 16], the performance of metallic nanoparticles decorated GOx/CNTs as an electrochemical filter for wastewater treatment had not been previously reported.

In this study, GOx/CNTs, AuGOx/CNTs and AgGOx/CNTs filters were synthesized through chemical approach and applied for the treatment of wastewaters. The structural properties of synthesized filters were studied by SEM and XRD analyses. Finally, electrochemical properties of filters were investigated for electro-oxidation of the tetracycline, phenol and oxalate.

## 2. MATERIALS AND METHOD

In order to synthesized the graphene oxide [17], 3 ml of  $\text{H}_3\text{PO}_4$  and 24 ml of  $\text{H}_2\text{SO}_4$  were stirred and mixed. Then, graphite powder (0.30 g) was added into the prepared solution under stirring condition. Potassium permanganate (1.40 g) was added gradually into the solution. The mixing solution was stirred for a few hours until the liquid became dark green. To remove the surplus potassium permanganate, 0.70 ml of hydrogen peroxide was dropped gradually and stirred for 12 min. The exothermic process took place and the mixture was let to cool. HCl (12 ml) and DI water (42 ml) was added and centrifuged for 6 minutes at 4000 rpm. The supernatant was poured out and the residuals were rewashed again with DI water and HCl for several times.

Graphene oxide solution ( $0.3 \text{ mg ml}^{-1}$ , 3 ml) was added to a solution of  $\text{HAuCl}_4$  ( $0.05 \text{ mg ml}^{-1}$ , 10 ml). After 30 minutes, the interaction of the gold ions with the graphene oxide surfaces was promoted. Then, the solution of sodium citrate ( $0.1 \text{ mg ml}^{-1}$ , 190 ml) was added as a reducing agent. After that, the solution was heated at  $90 \text{ }^\circ\text{C}$  for 3 hours. The solution was centrifuged (5000 rpm, 10 minutes) and washed with deionized water. Finally, the nanocomposites were dried through in an oven for 24 hours at  $90 \text{ }^\circ\text{C}$ .

Graphene oxide solution ( $0.3 \text{ mg ml}^{-1}$ , 3 ml) was mixed with  $\text{CH}_3\text{COOAg}$  solution ( $10 \text{ mg ml}^{-1}$ , 10 ml) and stirred at  $90 \text{ }^\circ\text{C}$ , followed by the addition  $\text{NaBH}_4$  solution ( $1 \text{ mg ml}^{-1}$ , 10 ml) and stirred quickly for 6 min at  $90 \text{ }^\circ\text{C}$ . Then, the mixture was stirred for 110 minutes at  $50 \text{ }^\circ\text{C}$ . After that, the

silver nanoparticle decorated graphene oxide nanocomposite samples were obtained by centrifugation (5000 rpm, 10 minutes) and washed with deionized water to remove any free silver ions. The washed nanocomposite solution was dried in an oven at 90 °C for 24 hours.

CNTs (NanoTechLabs, Yadkinville, NC) have a diameter of 15 to 20 nm and a 100 μm length. The anodic filters were produced by dispersing various weight ratio of GOx, AuGOx and AgGOx nanocomposite and CNTs at 0.5 mg mL<sup>-1</sup> total concentration into N-methyl-2-pyrrolidone by a probe sonication (VCX 750 750-Watt, Sonicator) for 20 minutes. 15 mL sonicated mixture of the prepared nanocomposite and N-methyl-2-pyrrolidone were vacuum filtered onto a 5.0 μm pore Polytetrafluoroethylene (PTFE) membrane (Millipore, Omnipore, JMWP) and washed with 100 ml of ethanol and DI water solution (volume ratio 1:1). In order to normalize the ionic conductivity and strength, 50 mM Na<sub>2</sub>SO<sub>4</sub> (inert electrolyte) was used.

All electrochemical electro-oxidation experiments using a perforated titanium (Ti) cathode were performed by a modified filtration. A 47 mm diameter GOx/CNTs, AuGOx/CNTs and AgGOx/CNTs anodic filters was supported by a polytetrafluoroethylene (PTFE) membrane were applied as anode and mechanical contact to a lead and Ti ring was used to directly connect to the power supply. A silicone o-ring and perforated sheet of Ti shim were applied for the separation of the electrodes and as the cathode, respectively. A modified 47-mm polycarbonate filter was used to incorporate both cathode and anode materials. The prepared filter was loaded into a filtration casing modified for electrochemistry. 50 mM Na<sub>2</sub>SO<sub>4</sub> was utilized as the background electrolyte, and ferrocyanide (Fe(CN)<sub>6</sub><sup>4-</sup>) solution was used as the model pollutant unless otherwise noted. The influent ferrocyanide electrolyte solution was peristaltically pumped (Masterflex) through the electrochemical filters. The electrodes were directly immersed in a beaker containing Fe(CN)<sub>6</sub><sup>4-</sup> solution (200 ml) and Na<sub>2</sub>SO<sub>4</sub> electrolyte (50 mM). The following equation (1) was used for the determination of the electro-oxidation or removal rate [18]:

$$RR_i = (C_{f,i} - C_{p,i}) \times J \quad (1)$$

where  $C_{f,i}$  and  $C_{p,i}$  are the concentration of the feed and permeate (M),  $J$  is the permeate flux (m<sup>3</sup> s<sup>-1</sup> m<sup>-2</sup>).

Chronoamperometry, DPV and EIS studies were carried out in the three-electrode cell which contains Ag/AgCl/(sat KCL), a Pt wire and carbon paste as a reference, counter electrode, and the working electrodes, respectively. Autolab modular electrochemical system (Eco. ChemieulTecht) was used for these studies. The 0.1 M phosphate buffer solutions were provided from H<sub>3</sub>PO<sub>4</sub> and NaH<sub>2</sub>PO<sub>4</sub>. The pH of the phosphate buffer solutions was adjusted by HCl and NaOH solution (pH Meter PCE-228HTE). EIS data (Solartron SI 1286) were recorded at 5 mV over a frequency range of 0.1 Hz to 100 kHz. Z-view software was used for the characterization of recorded EIS data.

Cyclic voltammetry (CV) measurements were done in -0.2 to 1 V potential range at a 10 mVs<sup>-1</sup> scan rate. Linear polarization measurements were carried out using a sweep rate of 0.01 V/s and a potential range from 0 to 2 V. The morphological structure of prepared GOx, AuGOx and AgGOx was analyzed by scanning electron microscopy (FESEM, Gemini Zeiss Supratm 35 VP, Carl Zeiss). Crystal structure prepared samples was performed with Xpert Pro X-ray diffractometer with 1.5404 Å (Cu Kα) in wavelength and 40KV/30 mA in power.

### 3. RESULTS AND DISCUSSION

Figure 1a shows the FESEM image of prepared GOx sample with the high density and high porosity of GOx. The characterizations of GOx can promote the physical and chemical absorption properties of filters. Figures 1b and 1c show the FESEM images of Au and Ag nanoparticles decorated GOx. Numerous Ag and Au nanoparticles are observed on the surface of GOx. Figure 1d shows the XRD pattern of GOx, AuGOx and AgGOx samples. XRD pattern of GOx gives a sharp peak at  $2\theta = 11.4^\circ$  whereby it is completely disappeared for other samples. Therefore, the functionalization of the GO surface with the Ag and Au nanoparticles might prevent the graphene sheets from restacking. The XRD patterns of AuGOx shows diffraction peaks at  $2\theta = 38.1^\circ, 44.3^\circ, 64.3^\circ$  and  $77.4^\circ$  that confirmed the presence of face-centered cubic (fcc) structured Au nanoparticles (JCPDS No 4-784) beyond the GOx structure. The attachment of Ag nanoparticles to the GOx structure exhibits the diffraction peaks at  $2\theta = 37.98^\circ, 44.2^\circ, 64.7^\circ$ , and  $77.8^\circ$  matched the crystalline planes of face-centered cubic silver (JCPDS No 07-0783).

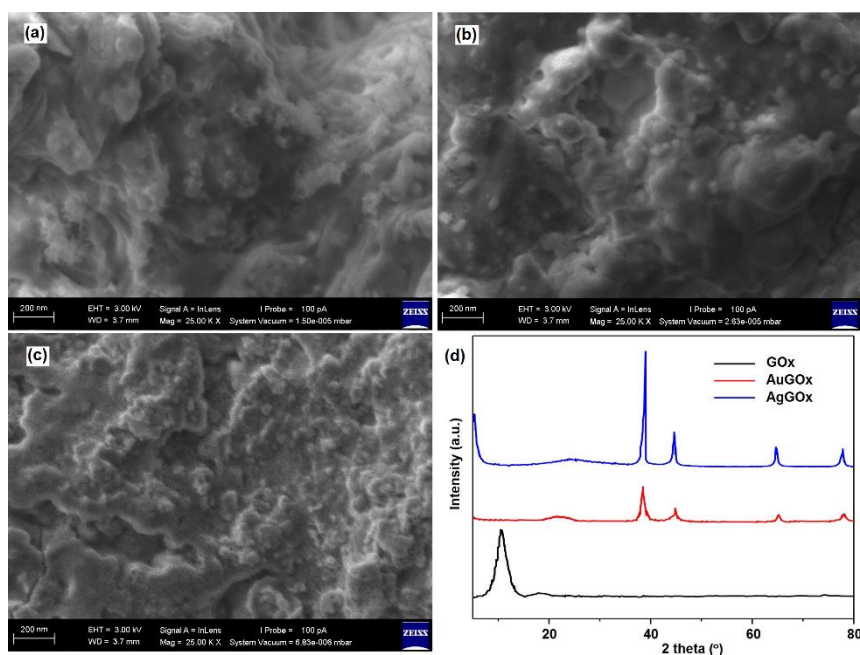


**Figure 1.** FESEM images of (a) GOx, (b) AuGOx and (c) AgGOx samples (d) XRD pattern of the samples.

In order to optimize the GOx/CNTs, AuGOx/CNTs and AgGOx/CNTs ratio, the measurements of electrical resistance of the filters are showed in Figure 2a. As seen, the electrical resistance of GOx/CNTs was the highest for 100% GOx filter ( $3006 \pm 110 \Omega$ ), and it was significantly decreased with the addition of CNTs. The maximum electrical resistance value of pure GOx can be related to low-connectivity between neighboring GOx particles [19]. Therefore, increasing the CNTs value in GOx filter can increase the electron hopping and electron conductance. It can be seen for AgGOx/CNTs samples that the electrical resistance of 100% AgGOx ( $6 \pm 0.3 \Omega$ ) have the minimum values because of the high electrical conductivity of Ag nanoparticles and penetrate the nanoparticle

on graphene structure. Figure 2a displays the addition of CNTs and the decrease of metallic nanostructures lead to an increase in the electrical resistance in AgGOx/CNTs and AuGOx/CNTs samples [7, 8].

For evaluation the prepared electrochemical filters,  $\text{Fe}(\text{CN})_6^{4-}$  was applied as an electron donor model. Figure 2b exhibits the electro-oxidation rate of 0.5 Mm  $\text{Fe}(\text{CN})_6^{4-}$  increased with increasing CNTs ratio from 0 to 40% for GOx/CNTs, AuGOx/CNTs and AgGOx/CNTs filters. Then, increasing the CNTs from 40 to 100% exhibits a reduction in the electrochemical performance. Therefore, ratio of 60:40 was considered as the optimal ratio for GOx/CNTs, AuGOx/CNTs and AgGOx/CNTs filters in the following electrochemical studies.

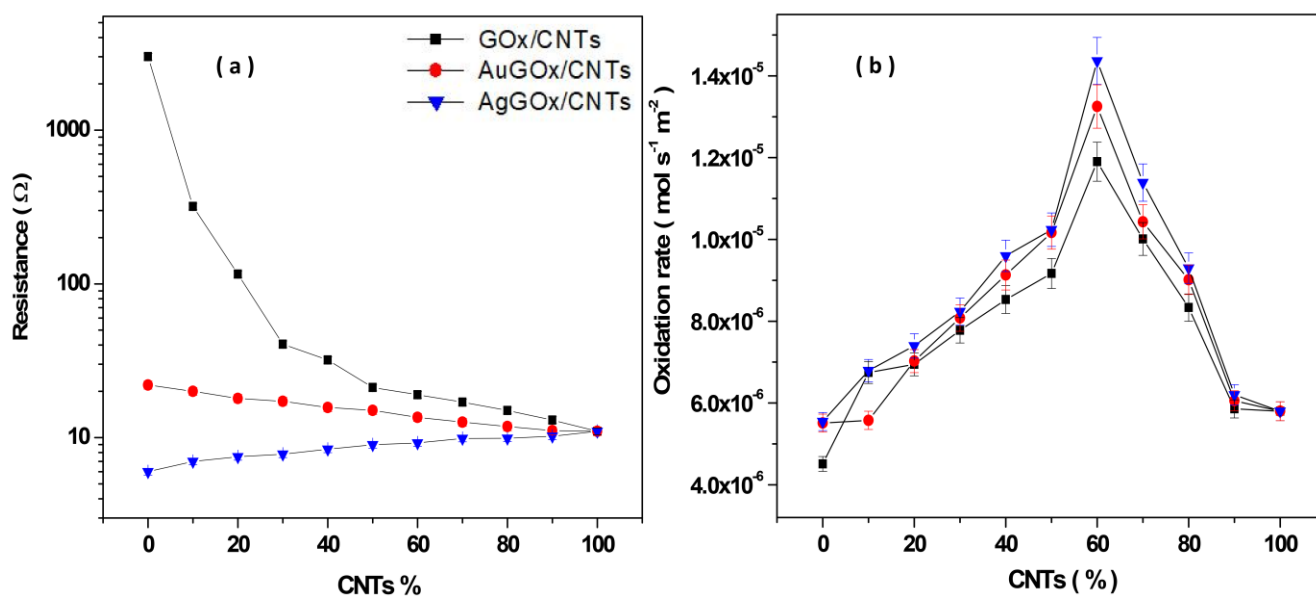


**Figure 2.** Effects CNTs contain in GOx/CNTs, AuGOx/CNTs and AgGOx/CNTs on (a) electrical resistance and (b) electro-oxidation rate of 0.5 mM  $\text{Fe}(\text{CN})_6^{4-}$  in 50 mM  $\text{Na}_2\text{SO}_4$  at anode potential of 0.5 V and 1.6 ml/minute flow rate.

In order to study the electro-oxidation property of prepared filters, effect of  $\text{Fe}(\text{CN})_6^{4-}$  concentration and anode potential were evaluated. Figure 3a-c shows the electro-oxidation rates of electrochemical GOx/CNTs, AuGOx/CNTs and AgGOx/CNTs filters for  $\text{Fe}(\text{CN})_6^{4-}$ . As seen, the electro-oxidation rates are increasing with the increase in the anode potential and the concentration of  $\text{Fe}(\text{CN})_6^{4-}$  for all filters. By considering the non-negligible value of electro-oxidation rates at anode potential of 0.12 V, it can be considered as the minimum over-potential for the oxidation process regardless of the types of filters and  $\text{Fe}(\text{CN})_6^{4-}$  concentrations. By increasing the anode potential from 0.12 to 0.5 V, the electro-oxidation rates were increased linearly. For anode potential above 0.5 V, voltage-independent plateaus are observed due to the mass transfer limitations [20]. As seen, increasing the influent concentration and internal electrode convection lead to an increase in the electro-oxidation rates.

To study the effect of influent concentration and anode potential, steady-state current electrochemical filtration of 0.5 and 5 mM of  $\text{Fe}(\text{CN})_6^{4-}$  are shown in Figure 3e-f. As seen, increasing

the anode potential leads to a growing steady-state current. It can be observed in low concentration potential independent mass transfer limited plateau for applied potential over 0.4 V. Furthermore, it is not exhibited in high concentration because of the domination mass transfer limitations in high diffusion rates. Therefore, by considering the electrochemical studies (the recorded DPVs and CVs in Figures 10 and 11) the following study on the electrochemical properties of filters was performed at the anode potential of 0.5 V.

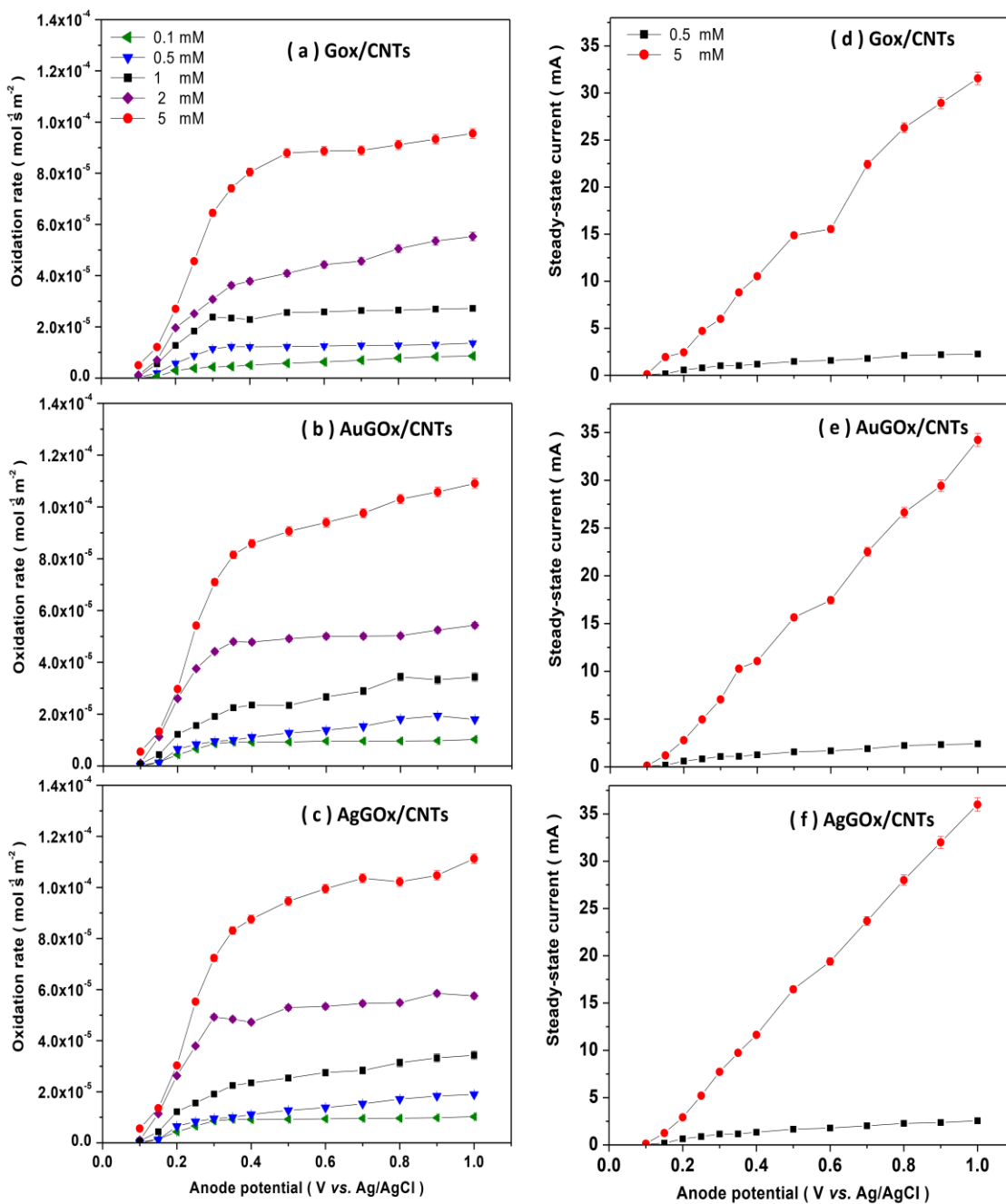


**Figure 3.** Effects of  $\text{Fe}(\text{CN})_6^{4-}$  concentration on (a-c) electro-oxidation rate and (e-f) steady-state current in GOx/CNTs, AuGOx/CNTs and AgGOx/CNTs filters in 50 mM  $\text{Na}_2\text{SO}_4$  at 1.6 ml/minute flow rate.

The chronoamperometry technique was applied to study the effect of internal electrode convection in 50 mM Na<sub>2</sub>SO<sub>4</sub> and at 1.6 ml/minute flow rate of influent 0.5 mM Fe(CN)<sub>6</sub><sup>4-</sup> at 0.5 V applied anode potential. Figure 4 shows the initial currents of the batch systems are about 3.83 mA and drop swiftly over the first few seconds to 0.65 mA as a steady-state current due to the expansion of electrochemical diffusion layer. Furthermore, the initial current of the electrochemical GOx/CNTs, AuGOx/CNTs and AgGOx/CNTs filters were recorded as 22.84, 27.51 and 28.65 mA, respectively. For these filters, the current was also reduced rapidly and there were a periodic oscillations to steady-state current of 2.02, 3.34 and 4.36 mA for GOx/CNTs, AuGOx/CNTs and AgGOx/CNTs filters, respectively. These Oscillations may be related to the periodic change in the flow rate from peristaltic pump. Increment in steady-state current for the graphene/CNTs based filters especially AgGOx/CNTs, illustrates that the molecular flux to the anode surface is remarkably increased by the internal electrode convection.

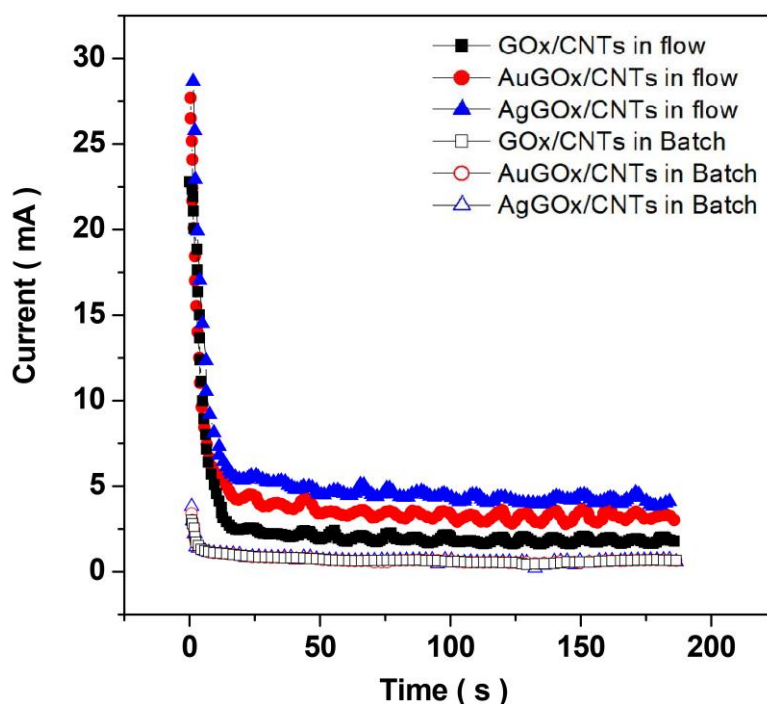


**Figure 4.** Chronoamperometry of GOx/CNTs, AuGOx/CNTs, AgGOx/CNTs in flow and batch systems of 0.5 mM Fe(CN)<sub>6</sub><sup>4-</sup> in 50 mM Na<sub>2</sub>SO<sub>4</sub> at anode potential of 0.5 V and 1.6 ml/minute flow rate.

Figure 5 illustrates the EIS and equivalent circuit model for the GOx/CNTs, AuGOx/CNTs and AgGOx/CNTs filters and batch systems. In these equivalent circuit model  $R_s$ ,  $R_f$ ,  $R_{ct}$  are solution resistance, film resistance and charge-transfer resistance, respectively [21].  $C_f$ , CPE and  $W_{mt}$  are film capacitance, double layer capacitance and mass transfer resistance, respectively. The results of EIS are presented in Table 1. Table 1 shows the calculated charge and mass transfer resistances of the graphene/ CNTs based filters are smaller than the batch system. The convection-enhanced mass transfer to the electrode surface can be observed[22]. Furthermore, the over-potential of mass transfer

was decreased by refilling the target molecule. Moreover, double layer capacitance values for the prepared graphene/CNTs based filters in this study were smaller than that in batch system because the convection may shorten the Debye length through induce near electrode surface refilling of target molecule.

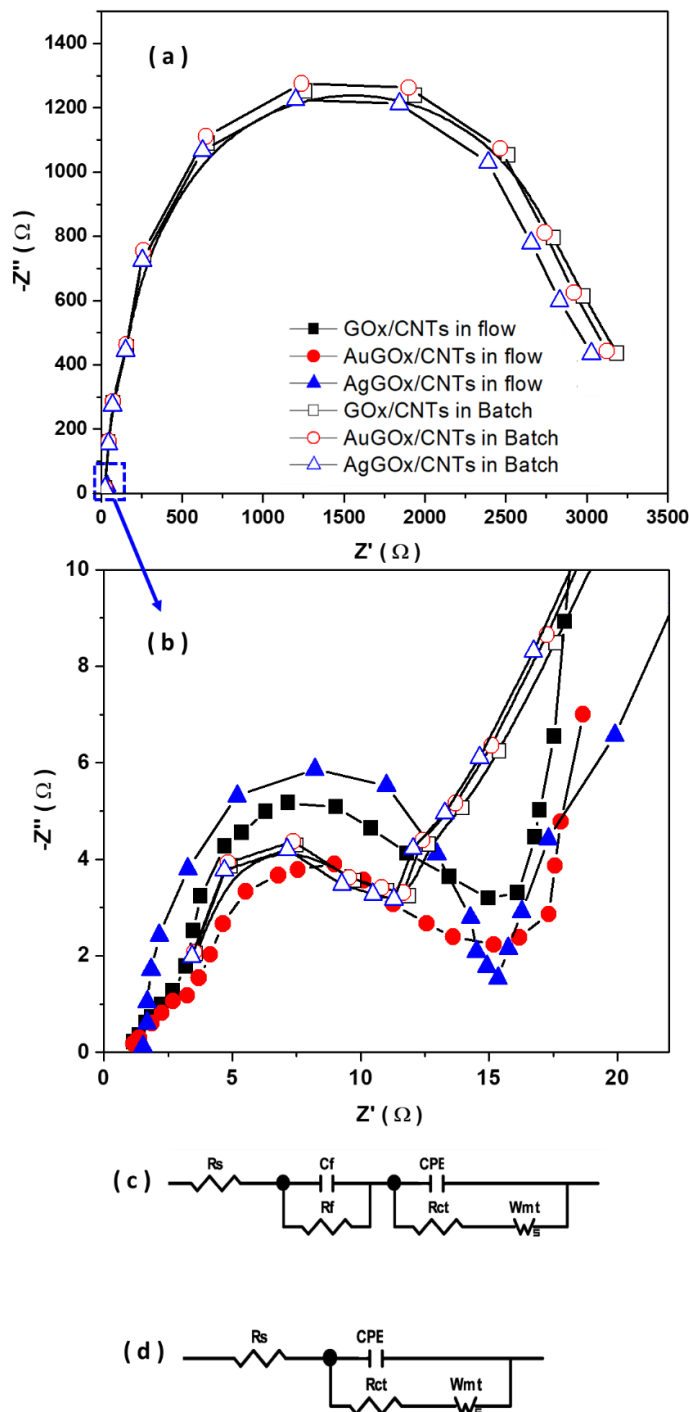


**Figure 5.** (a) and (b) EIS of GOx/CNTs, AuGOx/CNTs, AgGOx/CNTs and batch systems of 0.5 mM  $Fe(CN)_6^{4-}$  in 50 mM  $Na_2SO_4$  at anode potential of 0.5 V and 1.6 ml/minute flow rate. Equivalent circuit model for (c) batch and (d) flow systems of GOx/CNTs, AuGOx/CNTs, AgGOx/CNTs filters.

**Table 1.** Comparison of EIS analysis data in CNTs and graphene based electrode.

electrolysis conditions		$R_s$ ( $\Omega$ )	$C_f$ ( $\mu\text{F}$ )	$R_f$ ( $\Omega$ )	CPE ( $\mu\text{F}$ )	$R_{ct}$ ( $\Omega$ )	$W_{mt}$ ( $\Omega$ )	ref
GOx/CNTs, 50 mM $\text{Na}_2\text{SO}_4$ 0.5 V	flow batch	1.4 3.2	n/a 0.1	n/a 7.3	42.6 67.1	20.5 3350	188.2 417.7	This work
AuGOx/CNTs 50 mM $\text{Na}_2\text{SO}_4$ 0.5 V	flow batch	1.2 4.5	n/a 0.1	n/a 8.1	44.2 65.4	28.3 3285	177.5 411.2	This work
AgGOx/CNTs 50 mM $\text{Na}_2\text{SO}_4$ 0.5 V	flow batch	1.1 3.1	n/a 0.1	n/a 7.0	41.2 61.2	11.5 3215	165.1 400.1	This work
fresh CNT network 100 mM $\text{Na}_2\text{SO}_4$	flow batch	1.2 1.2	n/a 1.9	n/a 0.9	44.1 141.0	6.2 10.0	18.5 28.8	[23]
CNT network 100 mM $\text{Na}_2\text{SO}_4$ 0.82 V	flow batch	1.3 0.9	n/a 0.9	n/a 2.8	43.6 97.9	10.2 13.6	187.8 233.7	[23]
CNT network 100 mM $\text{Na}_2\text{SO}_4$ 2.10 V	flow batch	2.7 3.5	1.0 0.1	1.6 7.8	44.6 65.3	285.3 2992	n/a 431.3	[23]
GNP:CNT=70%:30% 10 mM $\text{Na}_2\text{SO}_4$ 0.4 V	flow batch	n/a n/a	n/a n/a	n/a n/a	250 15750	12 129.6	4.5 33.3	[20]

In order to investigate the penetration property and mass transfer performance of the prepared filters in the flow system, the observed rate constant kinetics of  $\text{Fe}(\text{CN})_6^{4-}$  oxidation ( $k_{\text{obs}}$ ) were determined as a function of penetration flux according to Yang et al. [24] and Guo et al. [25] studies. As seen in Figure 6, it is noticeable that the kinetics of  $\text{Fe}(\text{CN})_6^{4-}$  oxidation values of GOx/CNTs, AuGOx/CNTs and AgGOx/CNTs filters are plateauing at around 4.3, 4.5 and  $4.7 \times 10^{-4} \text{ m s}^{-1}$ , respectively. Therefore, it can be concluded that the oxidation process of  $\text{Fe}(\text{CN})_6^{4-}$  is controlled by kinetic limitation at a very high penetration fluxes. The measured values of kinetics of  $\text{Fe}(\text{CN})_6^{4-}$  oxidation in this study were at the highest in an electrochemical flow system compared to the reported value for  $\text{Ti}_4\text{O}_7$  and CNTs based filters [25, 26]. It can be related to the high porosity and the roughness due to the decoration of graphene oxide/ CNTs on polytetrafluoroethylene membrane by metallic nanoparticles in this study. The high porosity and roughness lead to more electro-active sites and high effective surface area for filters.

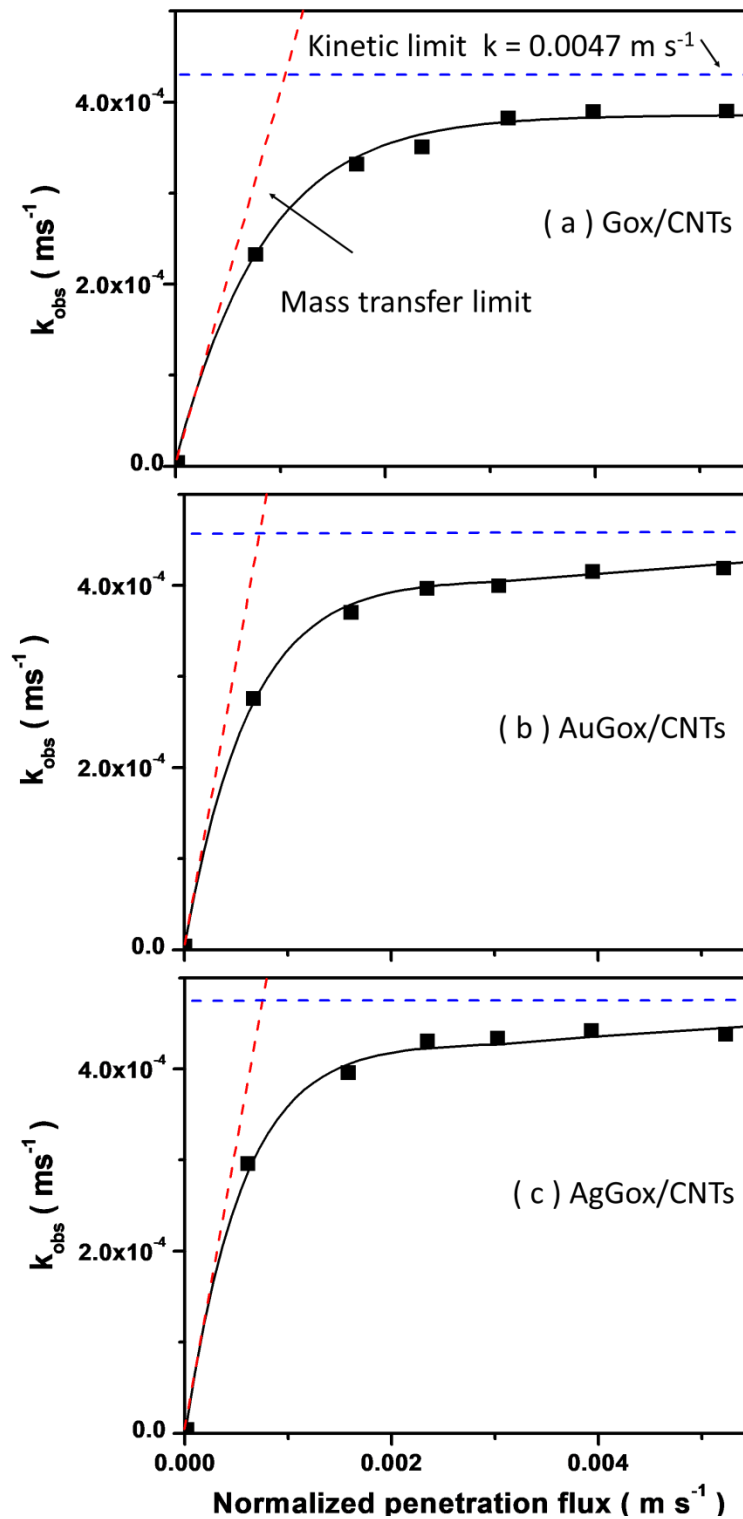


**Figure 6.** Plots of the normalized observed rate constant for  $Fe(CN)_6^{4-}$  oxidation for GOx/CNTs, AuGOx/CNTs and AgGOx/CNTs filters in flow system as a function of penetration fluxes. The blue and red dashed line are the normalized kinetic rate constant and the convective mass transfer limit, respectively.

In order to investigate the water treatment performance of GOx/CNTs, AuGOx/CNTs and AgGOx/CNTs filters, 0.1 mM tetracycline, 0.5 mM phenol and 0.5 mM oxalate were applied as influent. It should be considered that partial oxidation had taken place for the tetracycline and phenol because 106 and 28 electrons are needed to entirely anodic oxidization, respectively. Moreover, it is important point that PTFE membrane was able to adsorb trace organics but its active sites were saturated rapidly. On the other hand, the smaller resistance value of prepared graphene/CNTs based filters in this study showed desirable electro-oxidation rates than the pure graphene and pure CNTs filters. Figure 7 shows the electro-oxidation rates of tetracycline, phenol and oxalate. As seen, oxidation rates are very low at 0.1 and 0.2 V applied anode potential for three organic compounds. When the applied anode potential was increased, the electro-oxidation rates grew. For example, AgGOx/CNTs filter showed the electro-oxidation rates of tetracycline, phenol and oxalate were evaluated  $1.11 \times 10^{-5}$ ,  $2.11 \times 10^{-5}$  and  $2.19 \times 10^{-5} \text{ mol s}^{-1} \text{ m}^{-2}$  at 1.0 V, respectively. Strong interactions of planar aromatic of phenol with the aromatic graphene and CNTs structures had led to a higher electro-oxidation rates than the other components. It should be noted that increasing the anodic potential over 0.8 V had led to a decrease of filter efficiency because of the creation of gas bubbles on the electrode surface that damaged in filter structures.

Oxidation of tetracycline led to the formation of the side products and saturation the active site of filters [27]. Therefore, the suitable oxidation process of tetracycline was performed in the first 15 minutes of filter activity (more than 98%). By continuing the oxidation process, the removal efficiency of filter had decreased. Therefore, the first removal process during electrochemical filtration was oxidative degradation. No disturbance results on either permeability or electrochemistry were achieved after 90 minutes. As a consequence, the prepared graphene/CNTs based filters in this study indicated a proportionate stableness.

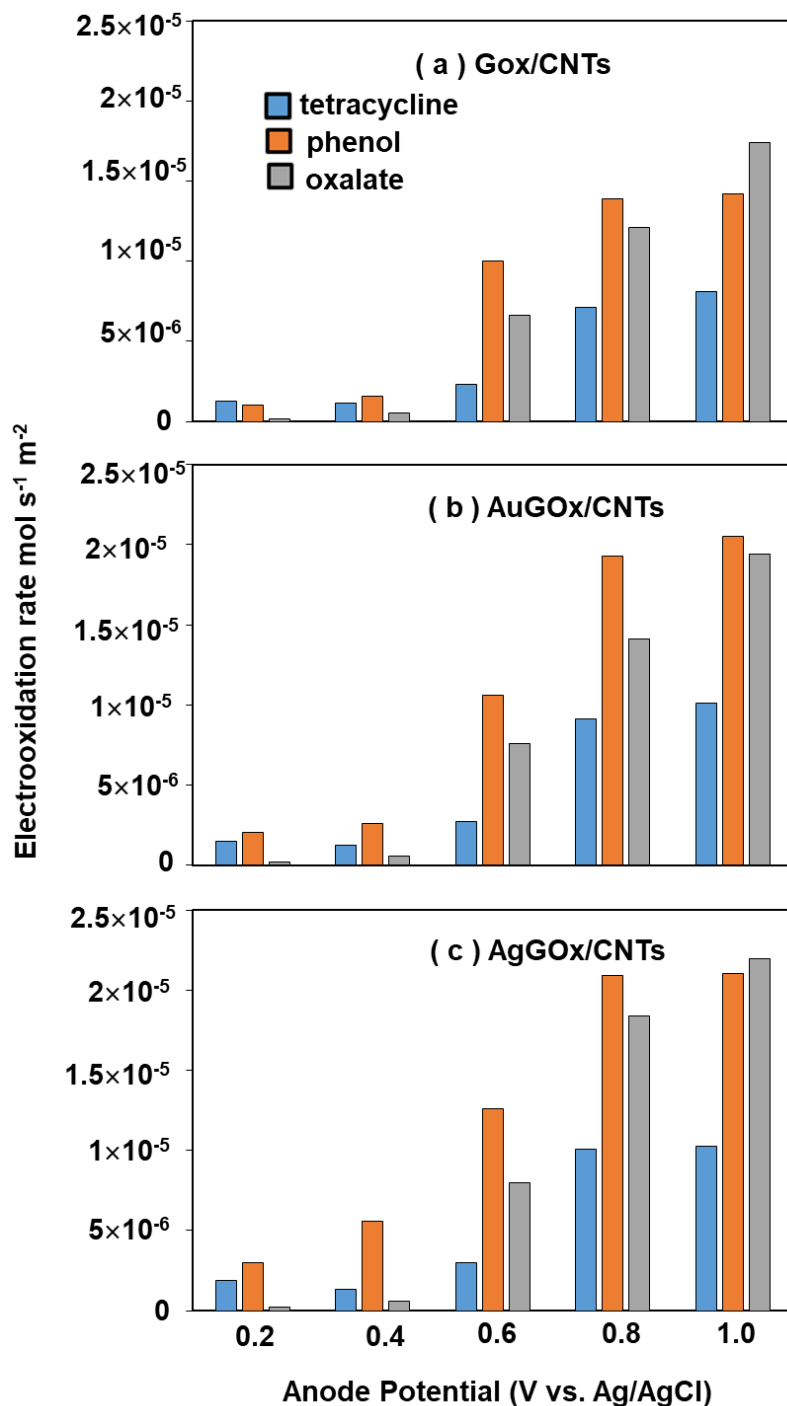


**Figure 7.** Electro-oxidation rate of 0.1 mM tetracycline, 0.5 mM phenol and 0.5 mM oxalate in (a) GOx/CNTs, (b) AuGOx/CNTs and (c) AgGOx/CNTs filters in 50 mM Na<sub>2</sub>SO<sub>4</sub> at 1.6 ml/minute flow rate.

The linear polarization curves of the GOx/CNTs, AuGOx/CNTs and AgGOx/CNTs filters are shown in Figure 8 and the oxygen evolution potentials are estimated 1.70, 1.82 and 1.90 V (vs. SCE) in neutral condition, respectively. The high oxygen evolution overpotential in filters are due to low side reaction of oxygen formation. Moreover, it can optimize the filtration performance of pollutants

during electro-oxidation operation of wastewater. Therefore, the AgGOx/CNTs filter shows the more suitable electrochemical efficiency than the other prepared filters.

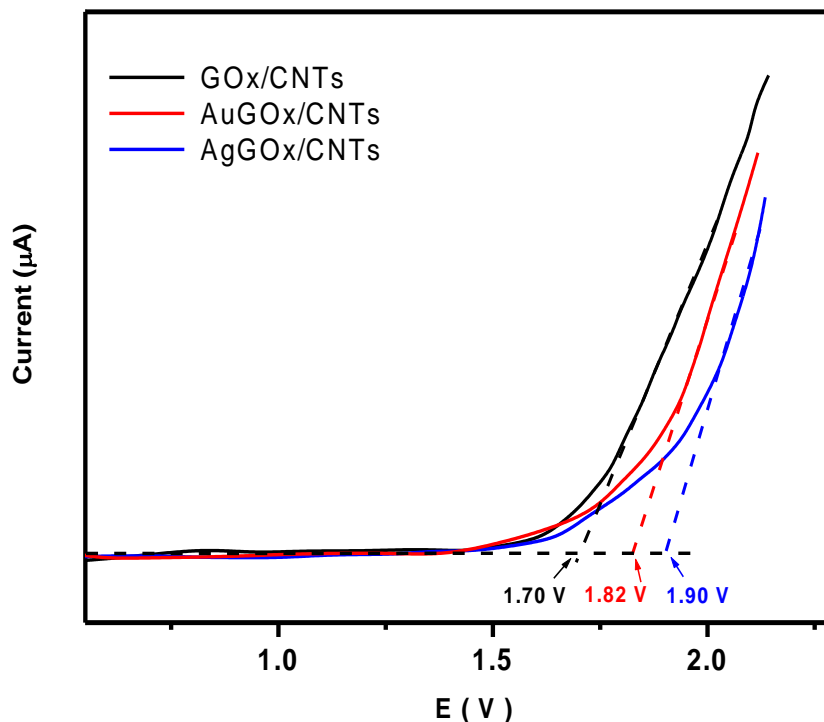


**Figure 8.** The linear polarization curves of GOx/CNTs, AuGOx/CNTs and AgGOx/CNTs filters at a scan rate of  $10 \text{ mV s}^{-1}$ .

To compare the phenol electrochemical filtration performance in real industrial and deionized water samples, two electrolytes were prepared. The deionized water was applied in the preparation of 0.1 M phosphate electrolyte solution (pH 7.0) as deionized sample and the river water (Xiangjiang River in Changsha, China) was applied for the preparation of 0.1 M phosphate electrolyte solution (pH 7.0) as real sample. Then, 0.5 mM phenol was added to both prepared electrolytes. Figure 9 displays the electro-oxidation rate of phenol in real water sample is similar to its electro-oxidation rate in deionized water especially for anodic potential over 0.4 V for all filter. To further examine this, a study was performed for 0.1 mM tetracycline and 0.5 mM oxalate and the electro-oxidation kinetics showed a similar property for both of real water and deionized water. Similarity in the results of AgGOx/CNTs filter is more than the other filters. It indicated that AgGOx/CNTs filter has better electro-oxidation properties than other prepared filters. Therefore, the following study on the removal performance of filters was performed on AgGOx/CNTs filter.

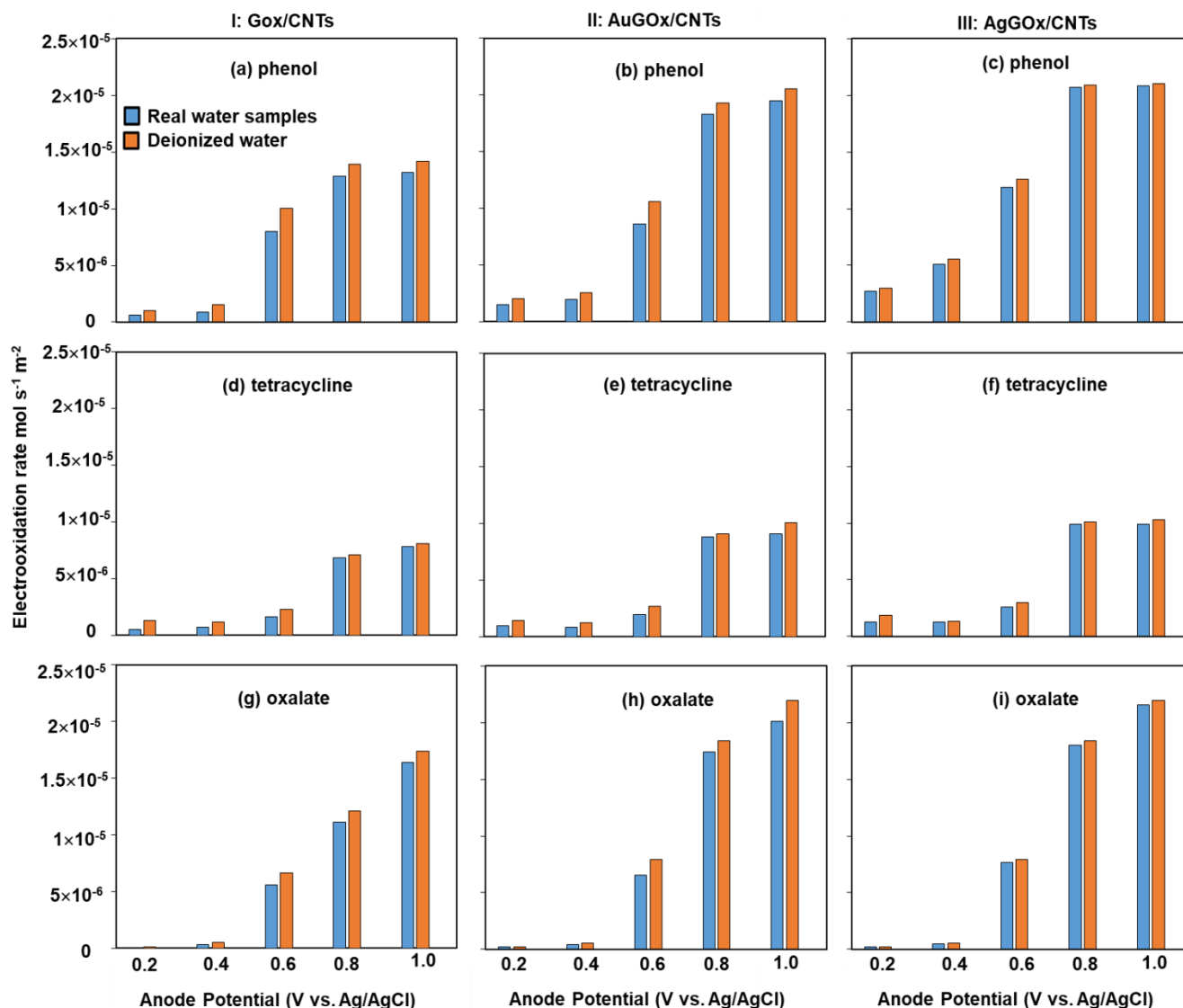


**Figure 9.** Electro-oxidation rate of 0.1 mM tetracycline, 0.5 mM phenol and 0.5 mM oxalate in real sample and deionized water column I: GOx/CNTs, II: AuGOx/CNTs and III: AgGOx/CNTs filters in 50 mM Na<sub>2</sub>SO<sub>4</sub> at 1.6 ml/minute flow rate.

The electrochemical filtration of 0.05 mM phenol in real water samples was recorded by differential pulse voltammetry (DPV) technique through the carbon paste electrode before and after the electro-oxidation with AgGOx/CNTs filter. Figure 10 shows the recorded DPVs of prepared buffer solution with deionized water (Figure 10a) and real sample (Figure 10b) in four conditions: without phenol, injection 0.05mM phenol before electro-oxidation, after 15 and 60 minutes electro-oxidation at 0.8 V. As seen, after 15 and 60 minutes electro-oxidation operation for the sample prepared in deionized water, 92% and 94% reduction of phenol is observed in electrochemical cell, respectively. 89% and 92% reduction of phenol is also observed for the sample prepared in river after 15 and 60 minutes electro-oxidation operation, respectively. It is consistent with the good removal activity of prepared filter for real samples.

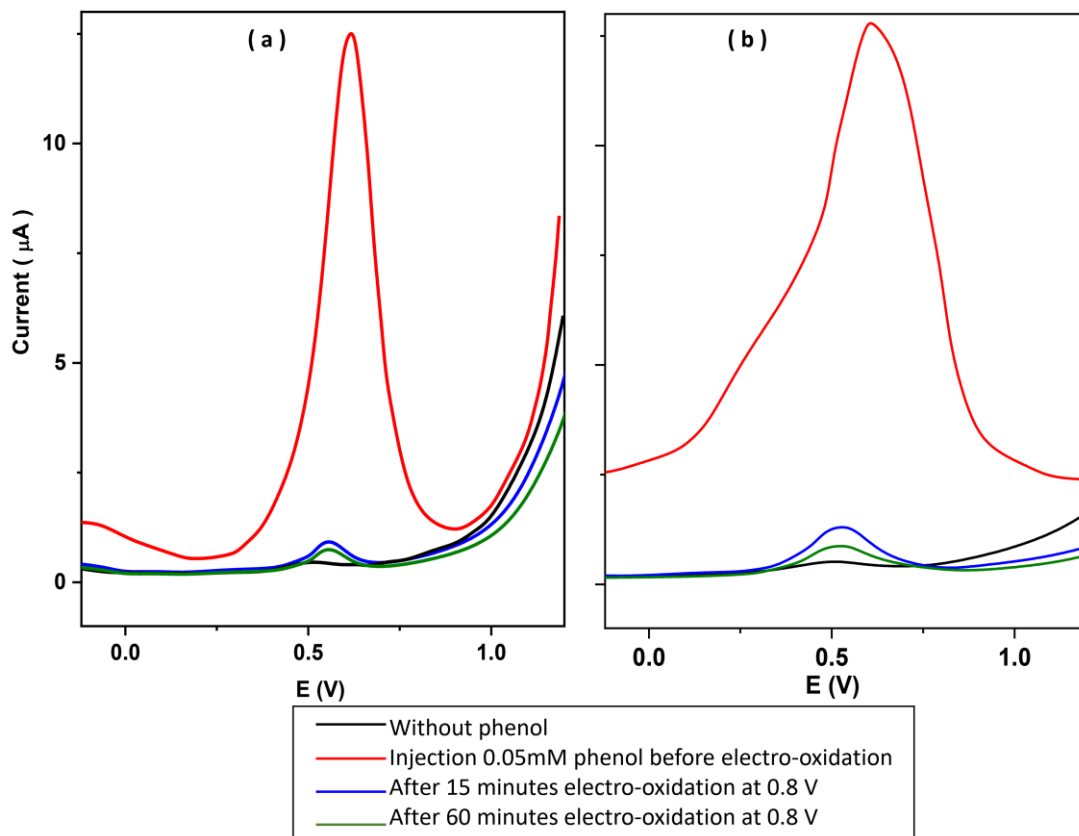


**Figure 10.** The recorded DPVs of carbon paste electrode in 0.1 M phosphate buffer solutions pH 7.0 at scan rate of  $10 \text{ mV s}^{-1}$  for the sample prepared with (a) deionized water and (b) real sample after and before of injection 0.05 mM phenol and after 15 and 60 minutes electro-oxidation operation at 0.8 V.

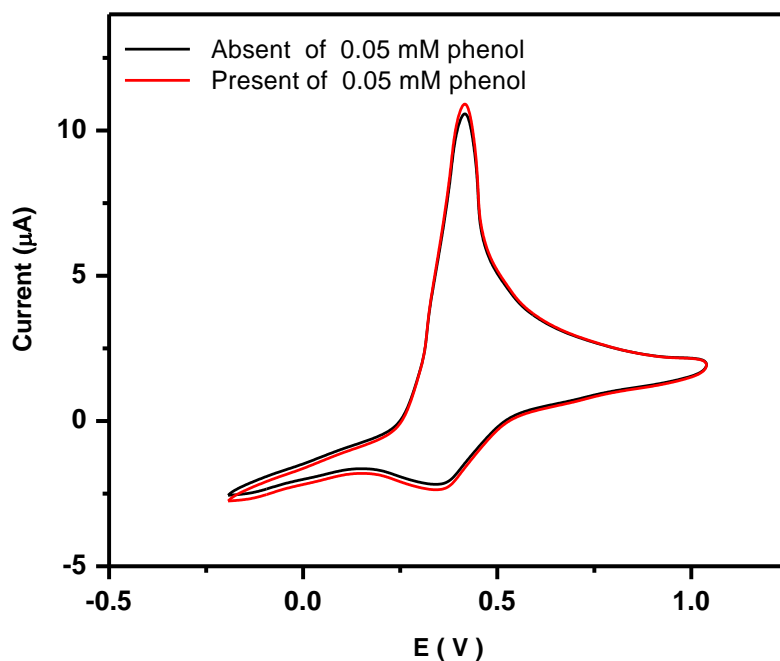


**Figure 11.** The recorded cyclic voltammograms of the AgGOx/CNTs filter at a scan rate of  $10 \text{ mV s}^{-1}$ .

In order to study the degradation effect of phenol in electrochemical properties of AgGOx/CNTs filter the cyclic voltammograms of the AgGOx/CNTs filter were recorded in the presence and absence of 0.05 mM phenol in 50 mM Na<sub>2</sub>SO<sub>4</sub> solution. As seen in Figure 11, addition of phenol in Na<sub>2</sub>SO<sub>4</sub> solution cannot create the additional peaks. It illustrates that the direct electro-oxidation of phenol did not take place over the AgGOx/CNTs filter. In addition, it can be deduced that the indirect hydroxyl radicals attack has a main role in electro-oxidation process of phenol which are electrochemically generated on the surface of an anode electrode [28].

#### 4. CONCLUSION

This study focused on the electro-oxidation properties of GOx/CNTs, AuGOx/CNTs and AgGOx/CNTs filters as wastewater treatment. The chemical approaches were applied for synthesis GOx and its decoration with Au and Ag nanoparticles. The structural properties of synthesized GOx/CNTs, AuGOx/CNTs and AgGOx/CNTs were studied by FESEM and XRD analyses. Electrochemical properties and removal properties of prepared filters were investigated for the treatment of tetracycline, phenol and oxalate from deionized water and real sample. Results of the morphology and structure studies showed high density of GOx, AuGOx and AgGOx with high effective surface area were synthesized. The fcc structured Au and Ag nanoparticles decorated on the surface of GOx structures. The result showed that AgGOx/CNTs filter exhibited a higher electro-oxidation rate than GOx, AuGOx filters. DPV technique was applied before and after the electro-oxidation of phenol in the river water. The results of DPV study showed that AgGOx/CNTs can be the proposed filter to remove phenol from real wastewater samples.

#### ACKNOWLEDGEMENT

This work was sponsored in part by National Natural Science Foundation of China (31471850), Science and Technology Plan Project of Science and Technology Bureau of Jingmen city, China (110588)

#### References

1. T. Veldkamp, Y. Wada, J. Aerts, P. Döll, S.N. Gosling, J. Liu, Y. Masaki, T. Oki, S. Ostberg and Y. Pokhrel, *Nature communications*, 8 (2017) 1.
2. A. Ahmad and R. Ghufuran, *International Journal of Sustainable Engineering*, 12 (2019) 47.
3. S. Touahria, S. Hazourli, K. Touahria, A. Eulmi and A. Aitbara, *International Journal of Electrochemical Science*, 11 (2016) 5710.
4. S. Evangelista, G. Viccione and O. Siani, *Journal of water process engineering*, 27 (2019) 1.
5. R. Hassanzadeh, A. Siabi-Garjan, H. Savaloni and R. Savari, *Materials Research Express*, 6 (2019) 106429.
6. J. Rouhi, C.R. Ooi, S. Mahmud and M.R. Mahmood, *Electronic Materials Letters*, 11 (2015) 957.
7. R. Savari, S. Soltanian, A. Noorbakhsh, A. Salimi, M. Najafi and P. Servati, *Sensors and Actuators B: Chemical*, 176 (2013) 335.

8. H. Savaloni, R. Savari and S. Abbasi, *Current Applied Physics*, 18 (2018) 869.
9. Q. Fu and X. Bao, *Chemical Society Reviews*, 46 (2017) 1842.
10. Z. Ji, T. Liu and H. Tian, *International Journal of Electrochemical Science*, 12 (2017) 7807.
11. V. Chabot, D. Higgins, A. Yu, X. Xiao, Z. Chen and J. Zhang, *Energy & Environmental Science*, 7 (2014) 1564.
12. H. Karimi-Maleh and O.A. Arotiba, *Journal of colloid and interface science*, 560 (2020) 208.
13. K. Yang, L. Feng, X. Shi and Z. Liu, *Chemical Society Reviews*, 42 (2013) 530.
14. F. Tahernejad-Javazmi, M. Shabani-Nooshabadi and H. Karimi-Maleh, *Composites Part B: Engineering*, 172 (2019) 666.
15. B. Bhanvase, T. Shende and S. Sonawane, *Environmental Technology Reviews*, 6 (2017) 1.
16. A. Khodadadi, E. Faghih-Mirzaei, H. Karimi-Maleh, A. Abbaspourrad, S. Agarwal and V.K. Gupta, *Sensors and actuators b: chemical*, 284 (2019) 568.
17. B. Paulchamy, G. Arthi and B. Lignesh, *J Nanomed Nanotechnol*, 6 (2015) 1.
18. C. Trellu, C. Coetsier, J.-C. Rouch, R. Esmilaire, M. Rivallin, M. Cretin and C. Causserand, *Water research*, 131 (2018) 310.
19. S. Changaei, J. Zamir-Anvari, N.-S. Heydari, S.G. Zamharir, M. Arshadi, B. Bahrami, J. Rouhi and R. Karimzadeh, *Journal of Electronic Materials*, 48 (2019) 6216.
20. Y. Liu, J.H.D. Lee, Q. Xia, Y. Ma, Y. Yu, L.Y.L. Yung, J. Xie, C.N. Ong, C.D. Vecitis and Z. Zhou, *Journal of Materials Chemistry A*, 2 (2014) 16554.
21. F. Husairi, J. Rouhi, K. Eswar, A. Zainurul, M. Rusop and S. Abdullah, *Applied Physics A*, 116 (2014) 2119.
22. C. Trellu, B.P. Chaplin, C. Coetsier, R. Esmilaire, S. Cerneaux, C. Causserand and M. Cretin, *Chemosphere*, 208 (2018) 159.
23. G. Gao and C.D. Vecitis, *ACS Applied Materials & Interfaces*, 4 (2012) 6096.
24. K. Yang, H. Lin, S. Liang, R. Xie, S. Lv, J. Niu, J. Chen and Y. Hu, *RSC advances*, 8 (2018) 13933.
25. L. Guo, Y. Jing and B.P. Chaplin, *Environmental science & technology*, 50 (2016) 1428.
26. N.G. Tsierkezos and U. Ritter, *The Journal of Chemical Thermodynamics*, 54 (2012) 35.
27. A.J. Jafari, B. Kakavandi, N. Jaafarzadeh, R.R. Kalantary, M. Ahmadi and A.A. Babaei, *Journal of Industrial and Engineering Chemistry*, 45 (2017) 323.
28. C. Barrera-Díaz, P. Cañizares, F. Fernández, R. Natividad and M. Rodrigo, *Journal of the Mexican Chemical Society*, 58 (2014) 256.